Journal of Integrative Neuroscience

J. Integr. Neurosci. **2026**; 25(8): 48170
https://doi.org/10.31083/JIN48170

Original Research

Chronic CeA^{CRH} Activation Disrupts Colonic IL-22/Reg3g Signaling and Induces Depression-Associated Microbiome Shifts in Male Mice

Liaorihong Zhao[1,2], Yu Long[3], Kexin Zeng[1], Shuya Chen[1,2], Tian Qiu[1,2], Ou Fu[1,2,*]

[1]School of Biotechnology, Jiangnan University, 214122 Wuxi, Jiangsu, China
[2]Laboratory of Food Perception Science, Science Center for Future Foods, Jiangnan University, 214122 Wuxi, Jiangsu, China
[3]School of Pharmaceutical Science, Zhejiang University of Technology, 310014 Hangzhou, Zhejiang, China
*Correspondence: fuou1031@jiangnan.edu.cn (Ou Fu)
Academic Editor: Robert J. McDonald
Submitted: 11 November 2025 Revised: 19 March 2026 Accepted: 3 April 2026 Published: 3 August 2026

Abstract

Background: Psychological stress shapes brain–body interactions through bidirectionally signaling between central neural circuits and peripheral systems. Central amygdala corticotropin-releasing hormone (CeA^{CRH}) neurons are key regulators of stress response and immune function. However, their chronic impact on the brain–gut–immune axis and gut microbiota remains poorly understood. **Methods**: We established a chronic stress model in mice by 14-day chemogenetic activating CRH neurons in the CeA. Behavioral assays were conducted to evaluate anxiety and depressive-like phenotypes. mRNA expression level of cytokines, tight junction proteins and antimicrobial peptide were compared in spleen or colon using qPCR between CeA^{CRH} activated group and control. In addition, 16S rRNA sequencing was performed to characterize changes in the microbial composition. **Results**: Chronic activation of CeA^{CRH} neurons showed a tendency toward anxiety-like behavior and significantly disrupts splenic and colonic immune homeostasis. Notably, the colonic interleukin-22 (IL-22)/regenerating islet-derived protein 3 gamma (Reg3g) mucosal defense axis was suppressed. Microbiota analysis revealed a shift toward a depression-associated profile, characterized by an increase in potentially pathogenic taxa (e.g., *Eggerthella* and *Actinomycetota*) and a reduction in short-chain fatty acid producers (e.g., *Ruminococcaceae* and *Roseburia*). These microbial alterations are consistent with clinical observations in patients with depression, supporting the translational relevance of mental disorders and gut microbiota. **Conclusions**: Chronic activation of CeA^{CRH} neurons drives coordinated immune, gut barrier, and microbiota alterations, including Claudin-2 upregulation and suppression of the IL-22/Reg3g axis, with IL-22 significantly reduced and Reg3g showing only a decreasing trend. These findings suggest a neuro–immune–microbiota pathway linking central stress circuits to peripheral dysfunction. Targeting IL-22 signaling, epithelial barrier integrity, or microbiota composition may represent promising therapeutic strategies for chronic stress-related disorders.

Keywords: central amygdaloid nucleus; corticotropin-releasing hormone; gastrointestinal microbiome; immunologic factors; antimicrobial peptides

1. Introduction

The central nervous system and peripheral immune systems are intimately interconnected through bidirectional neuroimmune communication [1,2,3,4]. Recently, studies focusing on the gut-brain axis and top-down regulation by the autonomic nervous system have revealed their active roles in this two-way dialogue [5]. In essence, the brain can influence peripheral immune activity (for instance, via stress-sensitive neural pathways and autonomic nerves [6]), as the peripheral immune system is innervated via sympathetic or parasympathetic efferents, and its cells express receptors for cholinergic or catecholaminergic neurotransmitters [1,7,8]. Conversely, changes in peripheral immune signals including inflammatory cytokines, which are caused by infection, gut impairment or diet-induced alteration of microbiota, can alter neural activity, mood, and social behavior [9,10]. Recent studies have also revealed how the brain integrates information on immunological and metabolic status [11] and exerts top-down control, such as promoting tissue-protective immune responses via reward circuitry [12]. Such neuroimmune communication is crucial for maintaining homeostasis and is implicated in various neuropsychiatric disorders when dysregulated [8,13].

In modern society, chronic psychological stress has emerged as a pervasive risk factor in daily life [14]. It is closely linked to the development of anxiety, depression, inflammatory bowel disease (IBD) [15], and other metabolic diseases. Stress can influence peripheral physiological function via the hypothalamic–pituitary–adrenal (HPA) axis and the autonomic nervous system [6], while also exacerbating inflammatory responses through impairment of immune system. Both preclinical and clinical studies highlight a key role for pro-inflammatory cytokines in stress-related mood disorders, including postpartum depression (PPD), where elevated levels of TNF-α, IL-1β, and IL-6 have been reported [16].

The central amygdala (CeA) is an integrative hub in valence detection to coordinate autonomic responses and

behavioral output toward aversive and appetitive stimuli [17,18]. In particular, it responds rapidly to aversive stimuli such as fear [19] and pain [20], mediating anxiety-like behaviors and physiological stress responses via neuromodulators such as corticotropin-releasing hormone (CRH) [21]. During fear learning, CeA circuits gate salience and plasticity and prominently organize defensive actions. Beyond emotional regulation, the CeA is now recognized to influence peripheral inflammation [22]. Recent studies also uncovered a direct neural–immune circuit linking the CeA to the spleen via sympathetic projections. Specifically, CRH neurons in the CeA and in the paraventricular nucleus (PVN) drive this pathway and regulate spleen immune activity [23]. Another study showed that under chronic stress, overall neuronal activity in the CeA is associated with the impairment of Brunner's gland function and the alteration of gut microbiota composition [24]. In parallel, accumulating evidence supports reciprocal interactions between stress and the gut microbiota [9,25]: microbial composition shapes anxiety- and depression-like behaviors [21,26], as shown by fecal microbiota transplantation studies [27], while stress-related brain activity can perturb gut physiology and microbial ecology. However, the precise role of CeA^{CRH} neuron in chronic stress and how it influences the peripheral immune system and gut microbiota remain unknown.

Here, we focus on CeA^{CRH} neurons in stress-related peripheral regulation. Chronic chemogenetic activation of these neurons induced a modest increase in anxiety level and disrupt immune homeostasis, accompanied by suppression of protective mucosal pathways (IL-22/Reg3g) and modulation of splenic immune activity. This was also associated with increased Claudin-2 expression in colon, indicative of impaired gut barrier integrity. Furthermore, microbiota profiling revealed shifts in bacterial taxa linked to depression and chronic stress. Collectively, our findings highlight a CeA^{CRH}–driven neuroimmune–microbiota axis that may contribute to the pathophysiology of stress related psychiatric and gastrointestinal disorders.

2. Materials and Methods

Detailed methods are presented in **Supplementary Materials**.

2.1 Animals

All procedures and experiments on animals were performed according to the guidelines of Institutional Animal Care and Use Committees of Jiangnan University (Wuxi, Jiangsu, China). 12 Male mice (8 weeks) were used: CRH-ires-cre (B6(Cg)-CRHtm1(cre)Zjh/J, Jackson Laboratory stock, 012704). Animals were group housed, up to four per cage, in a temperature (23 °C) and humidity (55%) controlled environment in standard cages on a 12:12 h light/dark cycle with ad libitum access to food and water. After experiments, animals were deeply anesthetized with 4% isoflurane (R510-22-10, RWD, Shenzhen, Guangdong, China) and euthanized by rapid cervical dislocation.

2.2 Chemogenetic Activation of CeA^{CRH} Neurons

To activate CRH neurons in central amygdala, Cre-dependent AAV2/9-hSyn-DIO-hM3Dq-mCherry (5×10^{12} vg/mL, S0192-9, Taitool, Shanghai, China) was bilaterally injected into the central amygdala (CeA) under stereotaxic guidance (anteroposterior (AP): −1.2 mm, mediolateral (ML): ±2.7 mm, dorsoventral (DV): −4.5mm from bregma). At each target site, 150 nL of viral solution was delivered at a rate of 70 nL/min using a Hamilton microsyringe (Neuros 7001, Reno, NV, USA) connected to a microinjection pump (LEGATO 130, KDS, Holliston, MA, USA).

For chemogenetic activation, deschloroclozapine (HY-42110, MedChemExpress, NJ, USA) was dissolved and administered intraperitoneally at a dose of 100 µg/kg body weight per day [28]. Control mice received saline.

2.3 Animal Habituation and Video Recording for Behavioral Test

Animals were habituated prior to assays. On day 12 and day 13, behavioral tests were performed 30 min after deschloroclozapine (DCZ) or saline injection. All sessions were recorded with a top-mounted camera (OSMO Action 5 Pro, DJI, Shenzhen, Guangdong, China).

2.4 Open Field Test

In open field test (OFT), mice were individually placed into the center of the testing box (0.4 m × 0.4 m × 1 m) and recorded for 5 min. Regions of interest (ROIs) were defined as follows: a peripheral zone (a 20-cm-wide band along all walls) and a center zone (a 20 cm × 20 cm square at the arena center). An entry into any ROI was scored when ≥60% of the animal's body crossed the boundary. For centroid-based tracking pipelines, an entry was alternatively defined when the body centroid entered the ROI.

2.5 Elevated Plus Maze

The elevated plus maze (EPM) consists of two open arms (30 × 5 × 25 cm) aligned with each other and perpendicular to the two closed arms (30 × 5 × 25 cm) in line with each other and a central area (5 × 5 cm). Mice were delivered to the center of the plus maze. The video was recorded for 5 min. The criteria for entry score are the same as those in OFT analysis.

2.6 Data Analysis for Behavior Test

Videos were analyzed using a pretrained DeepLabCut model to track major body points [29]. All analyses and plots were performed using Python 3.12 (Python Software Foundation, Beaverton, OR, USA) and Matlab2024a (MathWorks, Natick, MA, USA).

2.7 Intestinal Permeability Assay

FITC-dextran (FD4, Sigma-Aldrich, St. Louis, MO, USA) was used to test the gut permeability. Mice were deprived of food for 8 h prior to blood collection. FITC-dextran was dissolved in PBS at a concentration of 100 mg/mL and administered to each mouse (44 mg/100 g body weight) by oral gavage. Four hours later, mice were anesthetized with isoflurane and blood was collected from the retro-orbital sinus. Plasma was separated and measured in a black 96-well flat-bottom plate using a microplate reader (Ex 495 nm, Em 525 nm, SpectraMax ABS, Molecular Device, San Jose, CA, USA).

2.8 Perfusion and Immunochemistry

One hour after the final DCZ or saline injection, mice were anesthetized by i.p. injection of 1.25% Avertin (Tribromoethanol, M2910, 0.2 mL/10 g, Aibei Biotechnology, Nanjing, Jiangsu, China) during transcardial perfusion with PBS followed by 4% paraformaldehyde (PFA, H-80096618, Sinopharm, Shanghai, China). Coronal brain sections (50 µm) were prepared using a microtome (SM2010R, Leica Microsystems, Wetzlar, Germany) at about –20 ℃. Twelve to fifteen sections containing the CeA were selected for immunohistochemistry. Primary c-Fos antibody (1:7500, 226008, Synaptic Systems, Göttingen, Germany) was incubated for 48 h at room temperature. Then, PBST washed sections were incubated with secondary antibody (1:750, Alexa Donkey anti-guinea Pig IgG 488, Jackson ImmunoResearch, West Grove, PA, USA) for 2 h at room temperature in the dark. Finally, sections were covered with mounting medium containing DAPI (P0131, Beyotime, Shanghai, China). c-Fos–positive cells were automatically detected and counted with the a custom-made model called Cell Counting Network, and counts were summarized per brain region.

2.9 PAS Staining

Duodenum was fixed and dehydrated as mentioned above used for brain tissues. Samples were cryo-sectioned at 12 µm. Sections were then stained using the Periodic Acid Schiff (PAS) Stain Kit (C0142S, Beyotime, Shanghai, China) at bright field using a 20× lens.

2.10 Primers for RT-qPCR

All qPCR primers were designed on NCBI Primer-BLAST using standard parameters with specificity screening.

2.11 RNA Extraction, Reverse Transcription and Quantitative PCR

The spleen and colon were rapidly dissected and snap-frozen in liquid nitrogen. Total RNA was extracted using the RNA isolation kit (Vazyme R711, Vazyme Biotech, Nanjing, Jiangsu, China) according to the manufacturer's protocol. Complementary DNA was synthesized using the reverse transcription kit (AG11728, Accuracy Biology, Changsha, Hunan, China).

qPCR was performed on a QuantStudio 3 system (Thermol, Waltham, MA, USA) using the SYBR Green qPCR kit (AG11701, Accuracy Biology) in a 20 µL reaction volume. Cycling conditions were 95 °C for 10 s and 60 °C for 30 s, repeated for 40 cycles. All samples were run in duplicate on a 96-well plate.

2.12 RT-qPCR Analysis

Raw qPCR data obtained from the QuantStudio 3 systemwere analyzed in Microsoft Excel (Office LTSC 2021, Microsoft Corporation, Redmond, WA, USA). For each sample, technical duplicates were averaged; wells with duplicate SD >0.5 Ct were retested. β-actin was used as the internal reference gene. qPCR data were processed by calculating $\Delta Ct = Ct\_target - Ct\_reference$ and deriving $\Delta\Delta Ct$ by normalizing each sample's ΔCt to the control-group mean. Relative expression was expressed as fold change using the $2^{-\Delta\Delta Ct}$ method.

2.13 16S rRNA Sequencing

Colonic luminal contents were collected, snap-frozen, and processed for 16S rRNA profiling. The V3–V4 region was amplified with primers 341F/806R and sequenced on a NovaSeq 6000 system (Illumina, San Diego, CA, USA) in PE250 mode. Reads were processed in QIIME2 (Cutadapt adapter trimming; DADA2 denoising and chimera removal). Amplicon sequence variants (ASVs) were taxonomically assigned using a pre-trained SILVA v138 classifier. Downstream analyses included alpha and beta diversity with PCoA visualization. Between-group differences in community composition were tested by PERMANOVA (999 permutations). Differentially abundant taxa were identified using LEfSe (LDA ≥2.0) and Mann–Whitney U tests with FDR correction where appropriate. Phenotype and functional profiles were inferred using BugBase (https://bugbase.cs.umn.edu/) and FAPROTAX (https://pages.uoregon.edu/slouca/LoucaLab/archive/FAPROTAX/lib/php/index.php), respectively.

2.14 Statistical Analyses and Data Reproducibility

Statistical analyses were performed and graphs were generated using GraphPad Prism 8.0 (GraphPad Software, San Diego, CA, USA). For behavioral experiments, heatmaps and trajectory plots were generated in Python 3.12 using custom scripts. Data are presented as mean ± SEM, and statistical significance was set at $p < 0.05$. All the analyses were performed by experimenters blinded to the results.

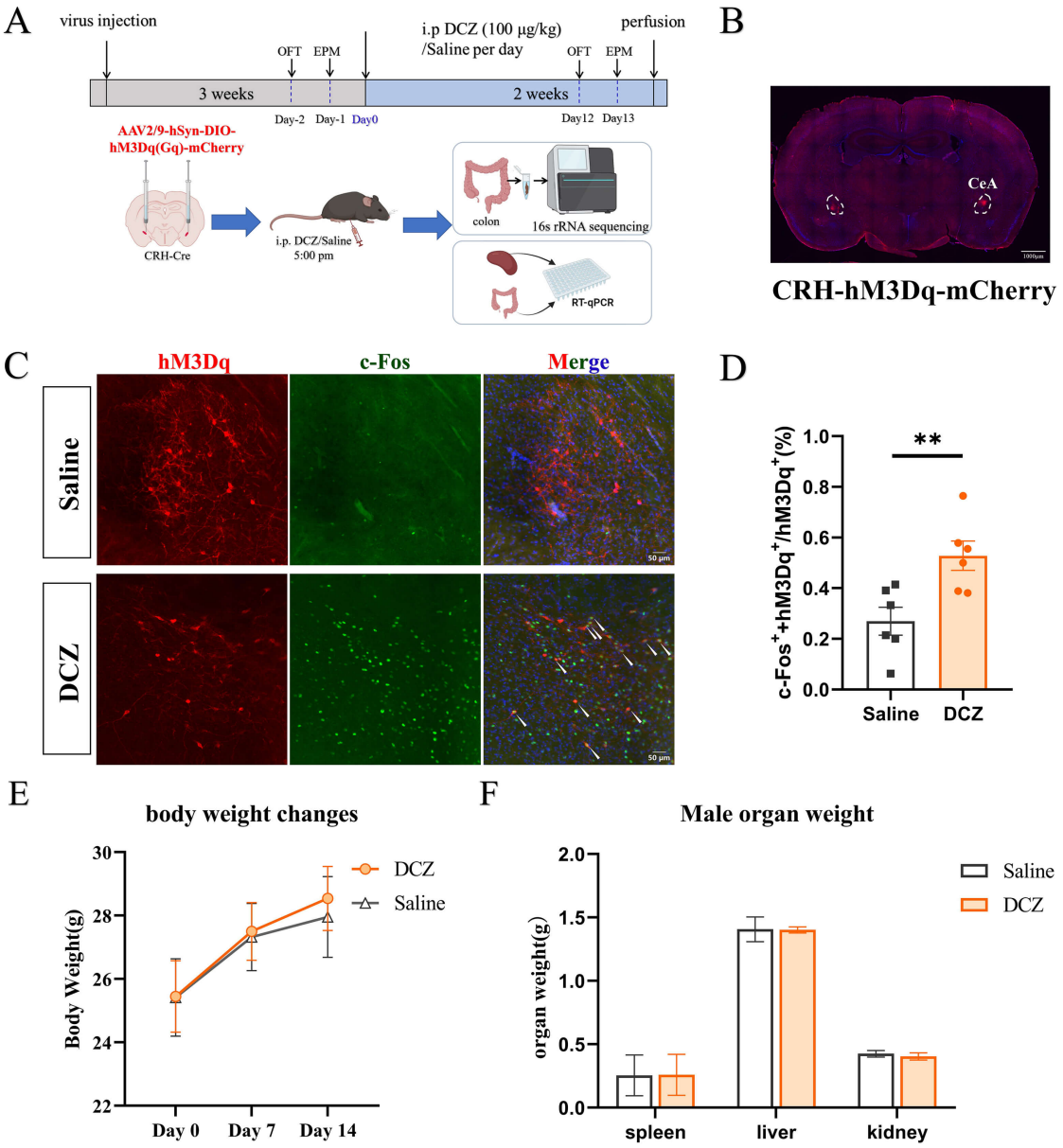

Fig. 1. Chemogenetic activation of central amygdala corticotropin-releasing hormone (CeA^{CRH}) neurons: experimental workflow, activation validation, and body/organ weights. (A) Schematic of experimental design and timeline. Male CRH-ires-Cre mice (n = 12) received bilateral CeA injections of AAV2/9-hSyn-DIO-hM3Dq-mCherry. After a 3-week expression period, mice were treated once daily for 14 days with DCZ (100 μg/kg, i.p.) (n = 6) or saline (n = 6). Open-field test (OFT) and elevated-plus maze (EPM) were performed on days 12–13, followed by tissue collection for 16S rRNA sequencing and RT-qPCR; a subset was perfused for histology. (B) Low-magnification coronal section showing hM3Dq-mCherry expression localized to bilateral CeA. Dashed box represents the CeA area. Scale bar, 1000 μm. (C) Representative CeA images from saline and DCZ groups: hM3Dq-mCherry (red), c-Fos (green), merged with DAPI (blue). Scale bar, 50 μm. (D) Quantification of neuronal activation ($c\text{-}Fos^{+}$ among $hM3Dq^{+}$ cells, %), showing increased activation in DCZ-treated mice relative to saline (unpaired *t*-test, t = 3.237, df = 9.970, $p = 0.009$, n = 6). (E) Body-weight trajectories over the 14-day treatment (2-way ANOVA, F_{time} (1.627, 16.27) = 24.85, $p < 0.001$; F_{drug} (1, 10) = 0.03145, $p = 0.8628$; $F_{time \times drug}$ (2, 10) = 0.2416, $p = 0.7877$, n = 6). (F) Endpoint organ weights (spleen, liver, kidney) in male mice (unpaired *t*-test; $t_{spleen} = 0.01991$, $df_{spleen} = 9.999$, $p_{spleen} = 0.998$; $t_{liver} = 0.05280$, $df_{liver} = 10.00$, $p_{liver} = 0.998$; $t_{kidney} = 0.5482$, $df_{kidney} = 10.00$, $p_{kidney} = 0.596$). Data are mean ± SEM; individual data points are shown (n as dots). Statistics: unpaired two-tailed *t*-test for (D,F); two-way ANOVA (treatment × time) for (E). $^{**}p < 0.01$. All comparisons not specifically annotated were non-significant (ns). (A) was created on BioRender (https://www.biorender.com).

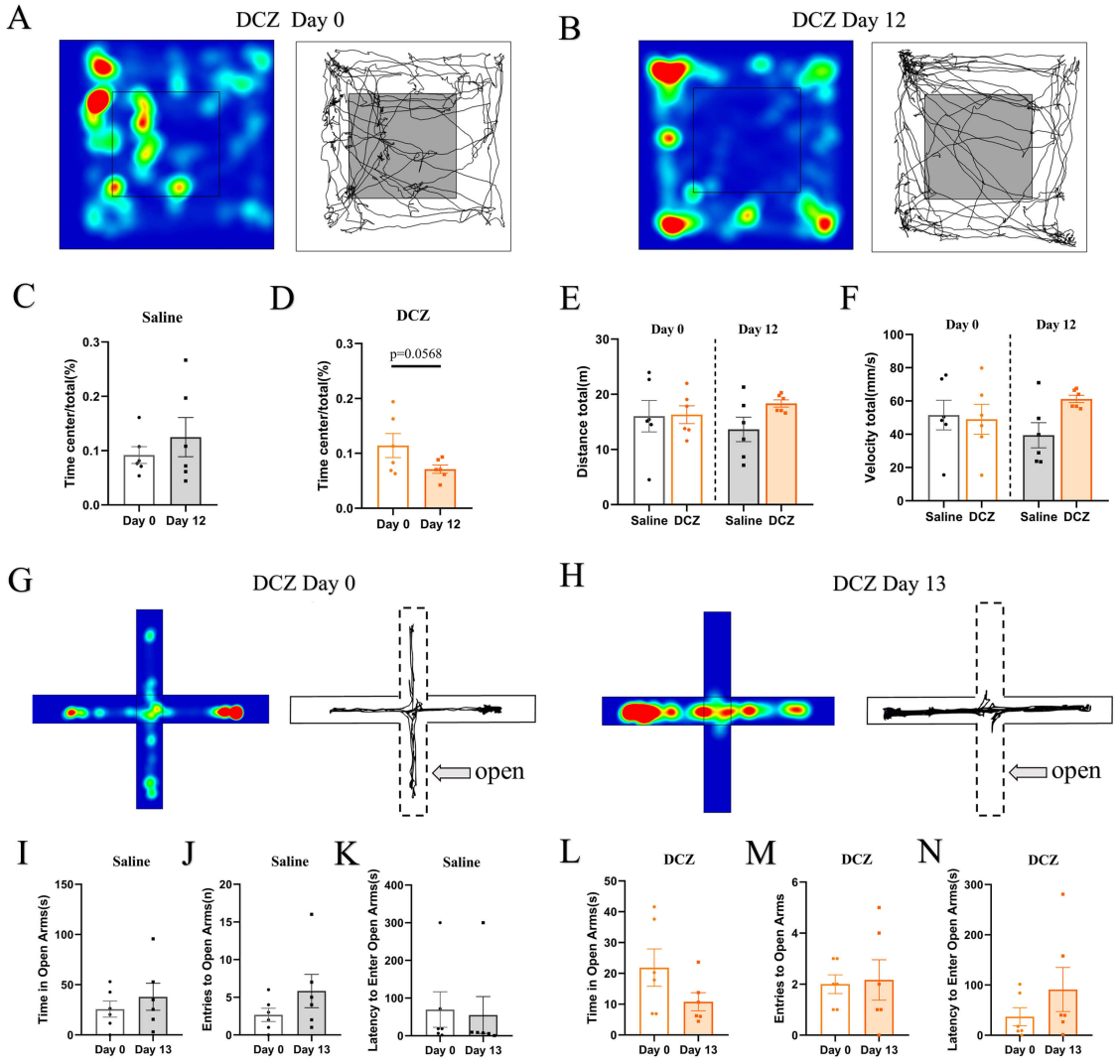

Fig. 2. Daily administration of DCZ in CeA CRH-hM3Dq mice increases anxiety levels. Open field Test (OFT). (A,B) Representative heatmaps (left) and trajectories (right) from the DCZ group at day 0 (A) and day 12 (B). (C) Time percentage in the center zone for saline (paired *t* test, t = 1.222, df = 5, $p = 0.276$, n = 6). (D) Time percentage in the center zone for DCZ groups at day 0 vs day 12. DCZ showed a reduction in center time with a trend toward significance (paired *t* test, t = 2.465, df = 5, $p = 0.0568$, n = 6). (E,F) Total travel distance (E, paired *t* test, $t_{saline} = 0.6648$, $df_{saline} = 10$, $p_{saline} = 0.521$; $t_{DCZ} = 1.17$, $df_{DCZ} = 10$, $p_{DCZ} = 0.269$) and mean velocity (F, paired *t* test, $t_{saline} = 1.036$, $df_{saline} = 10$, $p_{saline} = 0.324$; $t_{DCZ} = 1.321$, $df_{DCZ} = 10$, $p_{DCZ} = 0.216$) at day 0 and day 12 indicate no gross locomotor deficits. Elevated plus maze (EPM). (G,H) Representative heatmaps (left) and trajectories (right) from the DCZ group at day 0 (G) and day 13 (H). Dashed outlines indicate open arms. (I–K) Quantification for the saline group at day 0 vs day 13: time in open arms (I, paired *t* test, t = 0.7849, df = 8.146, $p = 0.455$), entries into open arms (J, paired *t* test, t = 1.330, df = 6.550, $p = 0.228$), and latency to first open-arm entry (K, Mann–Whitney U test, U = 12.50, $p = 0.418$). (L–N) Corresponding measures for the DCZ group: time in open arms (L, paired *t* test, t = 1.466, df = 5, $p = 0.203$), entries (M, paired *t* test, t = 0.1910, df = 5, $p = 0.856$), and latency (N, Mann–Whitney U test, U = 11, $p = 0.310$), consistent with increased anxiety-like behavior after chronic DCZ treatment. In EPM test, mice show an increased trend in anxiety-like behavior in DCZ-treated mice. Bars show mean ± SEM with individual mice as dots. All comparisons not specifically annotated were non-significant (ns).

3. Results

3.1 Chronic Chemogenetic Activation of CeA^{CRH} Neurons in CRH-Cre Mice Promotes Anxiety Like Behaviors

To selectively activate CRH neurons in the CeA, we bilaterally injected AAV2/9-DIO-hM3Dq-mCherry into the CeA of CRH-Cre mice (Fig. 1A). After 3 weeks of viral expression, mice received daily intraperitoneal injections of DCZ (100 μg/kg) for 14 consecutive days before the onset of the dark phase to chronically activate CeA^{CRH} neurons. To rule out nonspecific effects of viral expres-

sion or i.p. injection, control CRH-Cre mice received the same AAV injection but were administered saline instead of DCZ. We observed hM3Dq-mCherry expression in brain slices largely restricted to the CeA region (Fig. 1B) and c-Fos immunofluorescence staining was further performed to compare the neural activity level in these two groups. We found that in saline-treated control mice, only a small proportion of mCherry-positive CRH neurons expressed c-Fos, whereas DCZ-treated mice showed a markedly higher proportion (Fig. 1C). Quantitative analysis demonstrated that the percentage of c-Fos$^+$/hM3Dq$^+$ double-positive cells was significantly increased in the DCZ group compared with saline controls (Fig. 1D). These results confirmed that daily DCZ injection in CRH-hM3Dq mice reliably and specifically elevated basal activity of CeA^{CRH} neurons, allowing us to investigate their potential roles in neuropsychiatric disorders, neural-immune and brain-gut interactions. Moreover, we did not observe significant changes in body or organ weight (spleen, liver, and kidney) between DCZ-treated and control mice (Fig. 1E,F).

We next assessed the anxiety level and behavioral consequences of chronic CeA^{CRH} neuron activation using open field test (OFT) and elevated plus maze (EPM). Representative tracking plots in the OFT revealed reduced exploration of the center zone in DCZ-treated mice in day 12 compared with day 0 (Fig. 2A,B). Quantitative analysis showed a modest trend toward decreased time spent in the center zone ($p = 0.0568$, Fig. 2D), while saline-treated mice showed no significant changes (Fig. 2C). Importantly, total distance traveled and locomotor velocity were not different between groups (Fig. 2E,F), indicating that the observed changes were not due to impaired locomotor function. In the EPM, DCZ-treated mice exhibited a reduction in open arm exploration, including decreased time in open arms, prolonged latency to enter open arms, and fewer open arm entries (Fig. 2G,H,L–N) although these differences did not reach statistical significance. In contrast, saline-treated mice displayed minimal changes across these parameters (Fig. 2I–K). Together, these data suggest a tendency toward increased anxiety-like behavior following chronic activation of CeA^{CRH} neuron.

3.2 CeA^{CRH} Neurons Regulate Inflammatory Factor Levels in Spleen and Colon

We next investigated whether chronic CeA^{CRH} activation alters splenic immune function as a recent study suggests the spleen receives neural input from these neurons [22,23]. To assess these potential effects, we compared splenic cytokine levels in DCZ-treated and control mice. Our RT-qPCR analysis showed that mRNA levels of *Il6* and *Il12a* were significantly reduced, whereas *Tnf* was elevated in the spleen (Fig. 3A–E), suggesting that chronic activation of CeA^{CRH} neuron modulate splenic inflammatory responses by altering specific cytokine levels.

We next examined colonic cytokine levels in the colon as gut inflammation is often accompanied by neuropsychiatric disorders. Pro-inflammatory cytokines such as *Il1b* and *Tnf* were not significantly altered, while *Il6* exhibited a trend toward reduction ($p = 0.0828$, Fig. 3M). However, Il22/Reg3g axis showed a downward trend, but the change did not reach statistical significance ($p = 0.056$) in the DCZ group (Fig. 3F–Q), indicating compromised mucosal immune defense.

Next, we examined gut barrier function in CRH-hM3Dq mice, as stress has been reported to impair epithelial integrity and tight junction function in the colon. This prompted us to investigate whether CeA^{CRH} activation also affects the colonic permeability. RT-qPCR analysis showed that tight junction proteins, *Cldn1*, *Ocln*, and *Tjp1* exhibited no significant differences between groups, whereas *Cldn2* was significantly upregulated, suggesting increased colonic permeability (Fig. 3F–K). To functionally validate these findings, FITC-dextran assays were performed after 14 days of treatment. Plasma FITC levels measured 4 h after gavage showed a modest upward trend in DCZ-treated mice, further indicating increased colonic permeability (Fig. 3R). A recent study suggested that bulk activation neurons in CeA improves gut barrier integrity by promoting mucin release on duodenum [24]. However, our duodenal slices in CRH-hM3Dq mice did not show changes in mucin thickness but exhibited increased intercellular space in the DCZ group (Fig. 3S,T). Moreover, colonic *Muc1* and *Muc2* expression remained unchanged, indicating that mucus secretion capacity was not significantly altered by CeA^{CRH} activation (Fig. 3F,G). Taken together, chronic activation of CeA^{CRH} neurons may impair mucosal immune defense and increase colonic permeability, independent of central regulation of mucin release.

3.3 Gut Microbiome Analysis Reveals Depression-Related Taxonomic Shifts

As colonic immune protective function and permeability were altered in CRH-activated mice, we further assessed the impact of central stress signaling on the gut microbiome. We profiled colonic contents from DCZ-treated and saline mice using 16S rRNA sequencing. Alpha diversity analysis did not show significant changes across multiple indices (Shannon index, Sobs index, Pielou index, $p > 0.05$, Fig. 4B). Similarly, β diversity did not reveal a clear separation between the two groups by principal coordinate analysis (PCoA) and adonis test, suggesting that chronic chemogenetic activation of CeA^{CRH} neurons did not induce a large-scale remodeling of the gut microbiota (Fig. 4A). Both groups were dominated by Bacteroidota and Bacillota, along with common genera such as *Lactobacillus* and *Ileibacterium* (Fig. 4D,G).

While global diversity remained stable, we identified significant and selective shifts at the taxonomic level. Venn analysis confirmed that the vast majority of microbial lin-

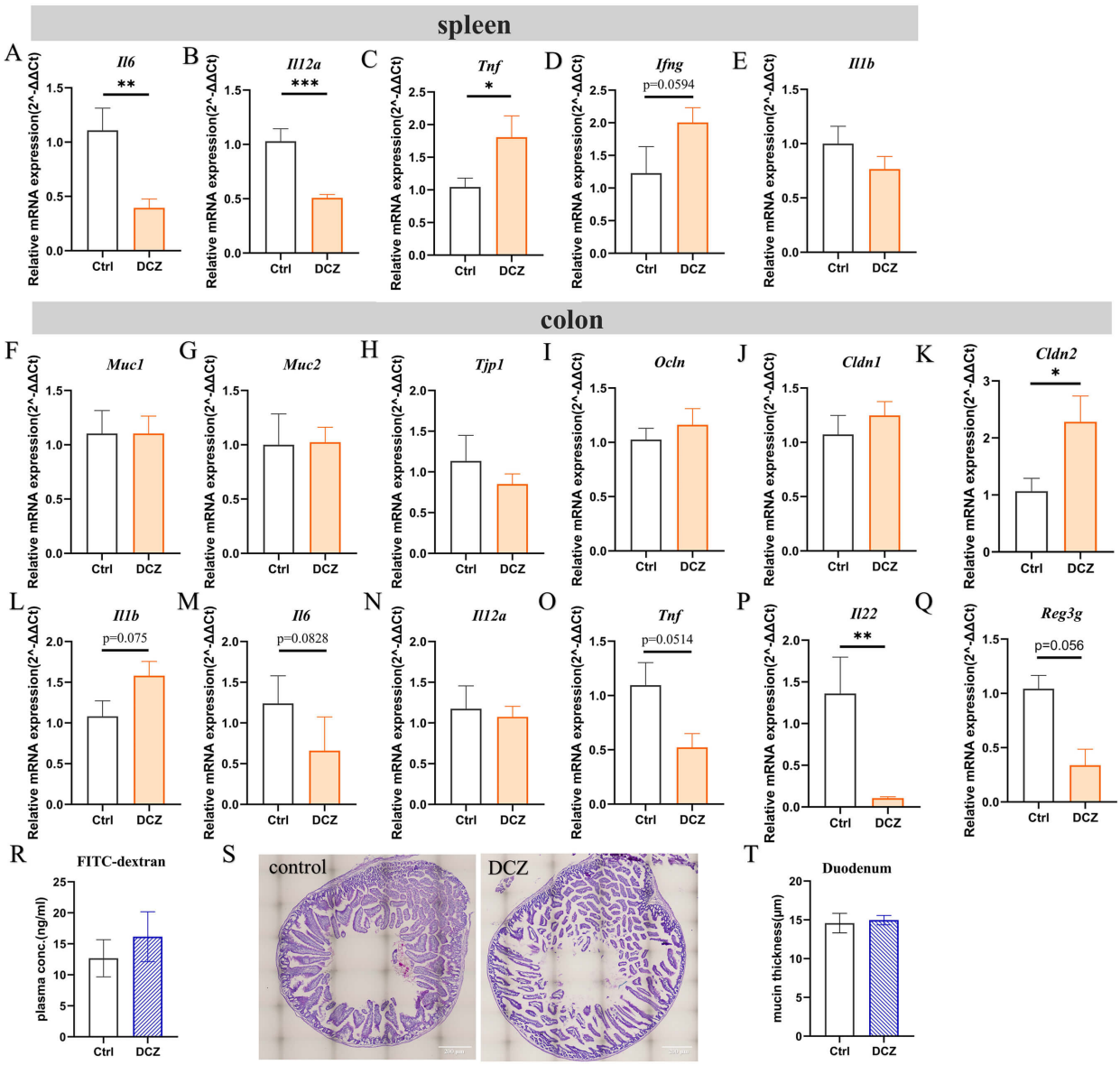

Fig. 3. Chronic CeA^{CRH} activation downregulates colonic IL-22/REG3G and upregulates CLDN2 with modest gut permeability and inflammatory changes in spleen and colon. (A–E) Spleen cytokines. *Il6* was decreased (unpaired *t*-test, t = 3.200, df = 9.743, p = 0.0098), *Il12a* was decreased (unpaired *t* test, t = 5.591, df = 7.919, p = 0.0005), *Tnf* was increased (unpaired *t* test, t = 2.438, df = 9.659, p = 0.0358), with trends for *Ifng* (unpaired *t* test, t = 2.261, df = 6.784, p = 0.0594) and *Il1b* (unpaired *t* test, t = 2.044, df = 7.940, p = 0.0705). (F–K) Colon epithelial barrier genes mRNA for *Muc1* (unpaired *t* test, t = 0.001333, df = 9.308, p = 0.9990), *Muc2* (unpaired *t* test, t = 0.4756, df = 8.359, p = 0.6465), *Tjp1* (Mann–Whitney U test, U = 17, p = 0.9372), *Ocln* (unpaired *t* test, t = 0.7532, df = 8.956, p = 0.471), *Cldn1* (Mann–Whitney U test, U = 13, p = 0.4848) showed no significant change, whereas Cldn2 was upregulated in DCZ mice (unpaired *t* test, t = 2.407, df = 7.329, p = 0.0454). (L–Q) Colon cytokines/defense genes. *Il1b* (unpaired *t* test, t = 0.8302, df = 9.507, p = 0.427), *Il6* (unpaired *t* test, t = 1.949, df = 9.085, p = 0.0828), *Il12a* (unpaired *t* test, t = 0.08788, df = 7.770, p = 0.483) did not show robust increase, *Tnf* showed a trend to rise (O, Mann–Whitney U test, U = 4, p = 0.0514), *Il22* was reduced (P, unpaired *t* test, t = 4.826, df = 5.589, p = 0.0035), and *Reg3g* showed a downward trend (Q, unpaired *t* test, t = 2.583, df = 4.367, p = 0.056). (R) Intestinal permeability assay: plasma concentration of 4-kDa FITC–dextran 4 h after gavage (Welch's *t*-test, t = 3.237, df = 9.970, p = 0.5068). (S) PAS staining of duodenum sections (representative images) illustrating mucosal morphology/goblet cell mucus. Left: Ctrl. Right: DCZ. Scale bar, 200 μm. (T) Mucin thickness assessed with PAS staining of samples from duodenum (unpaired *t*-test, t = 0.2786, df = 4.336, p = 0.7933). Bars show mean ± SEM with individual mice as dots (Ctrl vs DCZ). *p < 0.05, **p < 0.01, ***p < 0.001. All comparisons not specifically annotated were non-significant (ns). Mice were treated once daily for 14 days with DCZ (n = 6) or saline (n = 6).

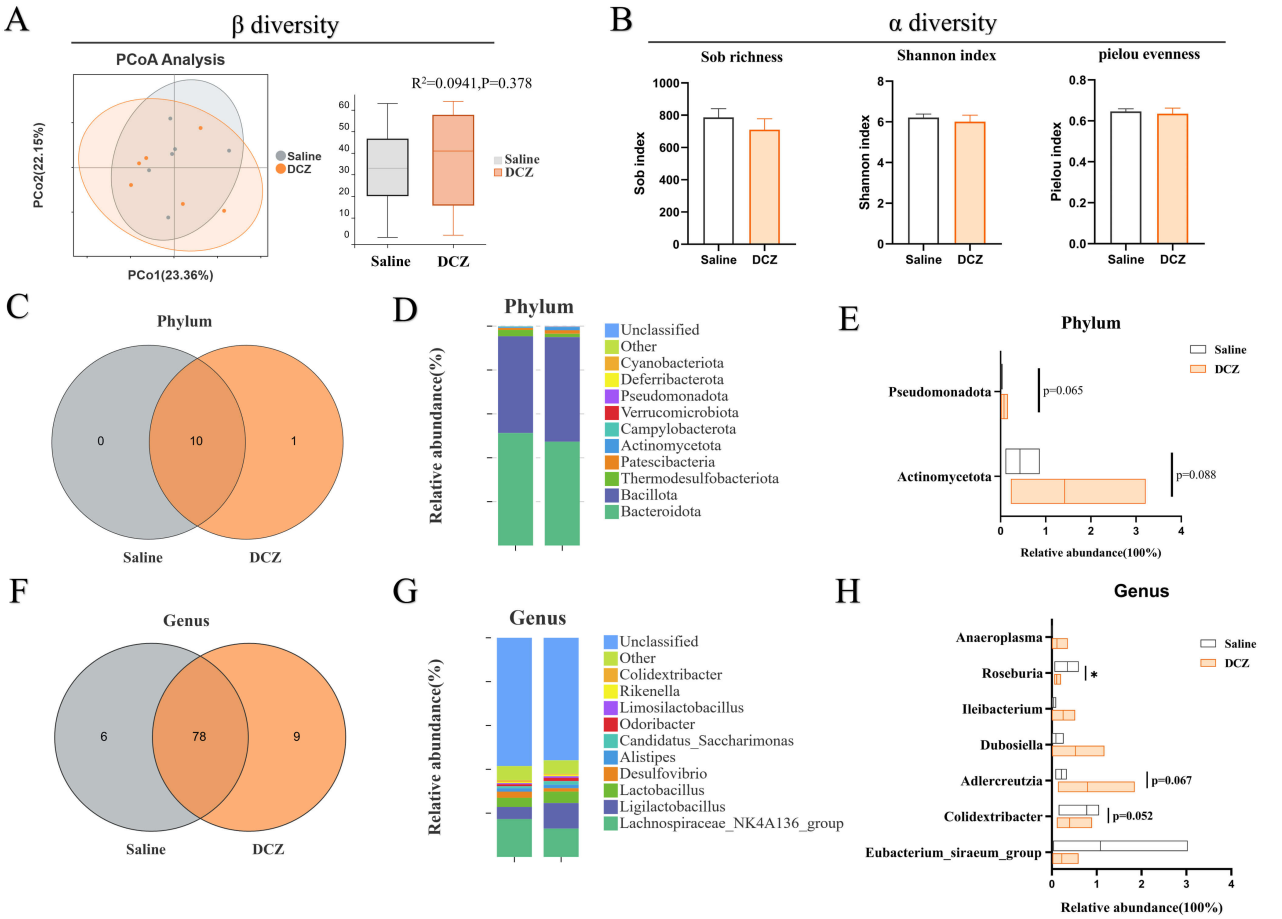

Fig. 4. Effects of chronic CeA^{CRH} activation on gut microbial composition. (A) β diversity. PCoA at the ASV level (Bray–Curtis). PERMANOVA indicates no significant group separation (R^2 = 0.0941, p = 0.378). (B) α diversity. Sobs richness (unpaired t-test, t = 0.8735, df = 9.562, p = 0.404), Pielou evenness (unpaired t-test, t = 0.3814, df = 6.940, p = 0.714), and Shannon index (unpaired t-test, t = 0.5552, df = 7.538, p = 0.595) show no significant differences between Saline and DCZ groups. (C,F) Shared taxa. Venn diagrams of detected phyla (C) and genera (F); most taxa are shared across groups with a small number unique to each condition. (D,G) Community composition. Stacked bar plots of relative abundance at the phylum (D) and genus (G) levels. (E) Differential phyla. (E) Group-wise comparisons for selected phyla in phylum level. Pseudomonadota and Actinomycetota show a trend toward difference (unpaired t test, t = 2.301, df = 5.477, $p_{Pseudomonadota}$ = 0.065, t = 2.057, df = 5.697, $p_{Actinomycetota}$ = 0.085). (H) Differential genera in genus level. Box plots for selected genera (*Anaeroplasma*, *Roseburia*, *Ileibacterium*, *Dubosiella*, *Adlercreutzia*, *Colidextribacter*, *Eubacterium_siraeum_group*). Other details are provided in **Supplementary Materials**. Mice were administered with either the drug or its vehicle. Saline group served as the control group for the respective experimental conditions. Bars/boxes show mean or median ± dispersion as appropriate. Statistics: unpaired two-tailed tests for taxa in (E,H). *p < 0.05. All comparisons not specifically annotated were non-significant (ns). PCoA, principal coordinate analysis; ASV, amplicon sequence variant. Mice were treated once daily for 14 days with DCZ (n = 6) or saline (n = 6).

eages were shared between the two groups (10 of 11 phyla and 78 of 93 genera; Fig. 4C,F), highlighting that the observed changes were confined to a limited set of taxa. At the phylum level, both Pseudomonadota and Actinomycetota exhibit a trend toward enrichment in DCZ-treated mice (Fig. 4E). Pseudomonadota is a well-established marker of gut dysbiosis [30] and a major source of Lipopolysaccharides (LPS). The expansion of this phylum may trigger a cascade of systemic inflammation [31]. Actinomycetota represents a major phylum of Gram-positive bacteria containing beneficial members (e.g., *Bifidobacterium*) and stress-associated pathobionts (e.g., *Eggerthella*). Its overall expansion is frequently identified as a microbial signature of major depressive disorder (MDD) in both clinical cohorts and rodent models [32,33]. Furthermore, at the genus level, three specific taxa showed significant shifts (Fig. 4H): *Anaeroplasma* and *Staphylococcus* wer increased, whereas *Colidextribacter* was depleted in the DCZ-treated group (*p*

= 0.052). *Staphylococcus* enrichment may reflect microbial responses to host neuroendocrine signals. These opportunistic pathogens can directly sense host-derived catecholamines (e.g., norepinephrine) and contribute to gut barrier disruption [34,35]. Recent studies have linked the expansion of *Colidextribacter* to increased oxidative stress and systemic inflammation in chronic stress models [36]. *Roseburia* is a well-characterized genus of anaerobic, butyrate-producing bacteria within the Lachnospiraceae family. It plays a critical role in maintaining intestinal homeostasis by providing essential energy to colonocytes and exerting anti-inflammatory effects [37]. The marked depletion of *Roseburia* is a recognized hallmark of stress-induced gut dysbiosis [38].

As alterations in gut barrier and inflammatory markers were observed, we next examined the association between microbial taxa shift and peripheral dysfunction. LEfSe analysis revealed that control mice were enriched for *Clostridium sp. Culture_41*, whereas DCZ-treated mice showed higher abundances of *Faecalibaculum*, *Staphylococcus*, *Anaeroplasma*, and related Acholeplasmataceae lineages (Fig. 5A–C), consistent with random forest test (Fig. 5I). Several of these taxa, notably Staphylococcus and *Anaeroplasma*, are considered stress-associated, suggesting that CeA-driven signaling facilitates their expansion.

Despite preserved overall composition at the phylum level (Fig. 4D–F), BugBase identified a single phenotype-level difference: the facultatively anaerobic phenotype was increased in DCZ mice, whereas Gram status, motility/biofilm potential, and stress tolerance function were comparable across groups (Fig. 5D,E). Decomposition of this phenotype further revealed group-specific contributors—the DCZ-associated increase was driven predominantly by Firmicutes (Bacillota) and Proteobacteria, indicating a redistribution of the taxa underpinning this phenotype relative to controls (Fig. 5F). Functional predictions further indicated targeted remodeling rather than global reprogramming: most modules were unchanged, but sulfur-compound metabolism pathways were selectively reduced (Fig. 5G, **Supplementary Fig. 1**).

Finally, we examined shifts in representative microbial taxa in our study, contextualizing our findings against existing literature on the association between gut microbiota and depression [39,40,41]. Interestingly, DCZ-treated mice exhibited similar trends in four taxa consistent with prior studies: an expansion of potentially pathogenic taxa (e.g., *Eggerthella* and *Actinomycetota*) and a reduction in short-chain fatty acid producers (e.g., *Ruminococcaceae*, and *Roseburia*) (Fig. 5H–J). This pattern suggests a potential role of CeA^{CRH} neurons in the development of depression-associated microbiota shift. Notably, random forest and indicator analyses specifically highlighted a marked decrease in the butyrate-producing genus *Roseburia*—a taxa consistently identified as a key feature in both depression and stress models (Fig. 5I,J) [41,42].

4. Discussion

Psychological stress is a major precipitating factor in anxiety, depression and other psychiatric disorders [15,43,44,45,46]. The CeA serves as a critical stress-integration hub [47], dynamically regulating the transition from adaptive to maladaptive responses depending on the duration and intensity of stress [23]. In this study, we employed a chemogenetic approach to chronically activate CRH neurons in the CeA, which mimics sustained psychological stress exposure. We demonstrated that, in addition to their roles in evoking anxiety, these neurons also exert downstream effects on the spleen-gut immune axis and alter gut microbiota. Our data suggest that chronic overactivation of CeA^{CRH} neurons causes a downregulated IL22/Reg3g–gut barrier function, Claudin-2-related impairment of gut permeability, and a mixed type of cytokine profile in the spleen—consistent with low-grade, autonomically tuned inflammation, thus pointing to a potential top-down mechanism underlying psychological stress induced peripheral dysfunction and microbiota alternation.

CeA^{CRH} neurons are responsive to mild aversive cues and are involved in the consolidation of fear memories [19,48,49]. In rodent models, selective activation of CeA^{CRH} neurons elevates anxiety-like behavior and impairs hippocampus-dependent memory, as reflected by poorer performance in the Y-maze and novel object recognition tests [21], mirroring core symptom domains observed in major depressive disorder (MDD) [50,51]. In our study, 14 days of CeA^{CRH} activation resulted in a modest tendency toward anxiety-like behavior without impairing locomotor activity, consistent with previous optogenetic and DREADD-based studies [52]. Different types of stress may also influence feeding behavior and metabolism [53,54,55]. Importantly, global CRH neuron activation across the brain for one week led to pronounced hypophagia and body-weight loss, reflecting systemic PVH^{CRH} induced HPA axis overactivation, although this phenomenon could also be induced by the CNO through daily food which can generate food-associated learning to avoid CRH activation [56]. In contrast, our CeA-specific CRH activation produced little change in body or organ weight, indicating that this modulation within limbic circuits does not directly affect feeding behaviors or systemic metabolism.

Spleen as the systemic immune organ, is also shown innervated by CeA by retrograde tracing using pseudorabies virus [57]. CeA GABAergic neurons can inhibit splenic Th2 responses through projections to the dorsal motor nucleus of the vagus (DMV) [22]. Another study focusing on CRH neurons in CeA and PVH, highlighting that optogenetic activation of these neurons can directly enhance immunity by promoting splenic plasma cell formation. Our qPCR analysis indicated that *Il6* and *Il12a* were decreased, whereas *Il1β* and *Tnf* were increased. This pattern suggests that while acute stress may enhance immune level in spleen as an adaptive response to threatening conditions,

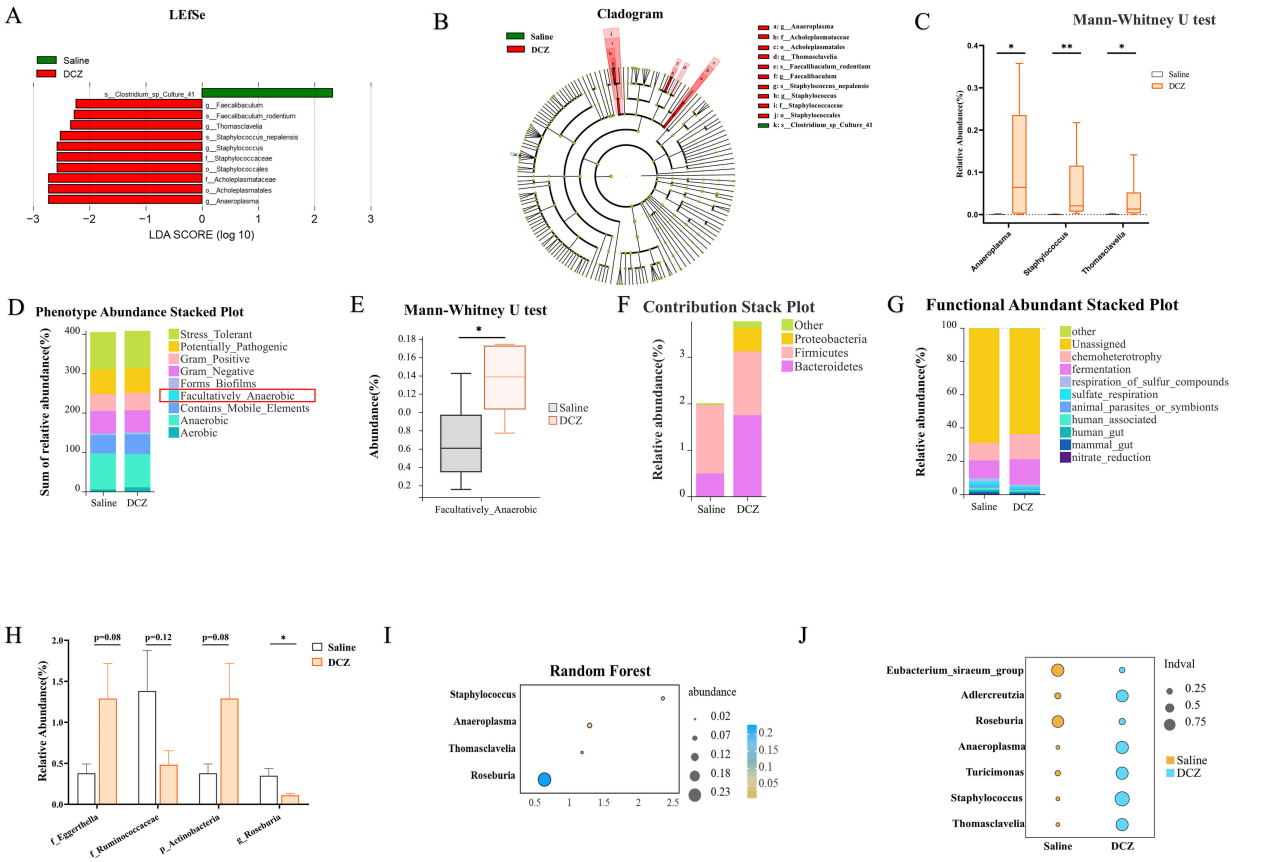

Fig. 5. DCZ-treated mice exhibited specific taxa changes related to depression. (A) LEfSe (LDA score, log10) highlighting taxa discriminating Saline (green) and DCZ (red) groups. (B) Cladogram of LEfSe results across phylum→genus ranks; red nodes indicate taxa enriched in DCZ, green in Saline. (C) Box plots of genera showing significant between-group differences (*Anaeroplasma*, *Staphylococcus*, *Thomasclavelia*). Groups were compared with two-tailed Mann–Whitney U tests (n = 6 per group); significance was determined (BH-FDR–adjusted q <0.05) unless otherwise indicated. Center line = median; box = IQR; Exact *p*/q values and multiple-testing details are provided in the **Supplementary Table 1**. (D) BugBase phenotype stack plot summarizing predicted community traits (e.g., Gram status, biofilm formation, stress tolerance, aerobic/anaerobic categories). (E) Wilcoxon rank–sum comparison for a selected phenotype (e.g., facultatively anaerobic) between groups (fold = 1.952469, p = 0.041126, q = 0.37013). (F) Taxonomic contributors to the highlighted phenotype in (E) at the phylum level (stacked composition). (G) FAPROTAX functional stack plot (e.g., fermentation, chemoheterotrophy, nitrate reduction, sulfur compound respiration), comparing Saline vs DCZ. (H) Bar plots compare the relative abundance of taxa previously closely linked to MDD (g_*Eggerthella*, f_*Ruminococcaceae*, p_*Actinomycetota*, g_*Roseburia*). Four taxa showed directionally concordant changes with prior MDD reports, presented as mean ± SEM with two-tailed p values. (I) Random-forest feature importance identifying top taxa discriminating groups (dot size encodes mean relative abundance). (J) Bubble plot of key taxa (e.g., *Eubacterium siraeum group*, *Adlercreutzia*, *Roseburia*, *Anaeroplasma*, *Turicimonas*, *Thermosediminibacter*), showing group means (x-axis), taxa (y-axis), and relative abundance (bubble size). Bars/boxes show mean or median with dispersion; dots are individual samples. Mice were administered with either the drug or its vehicle. Saline group served as the control group for the respective experimental conditions. Statistics: LEfSe (α = 0.05, LDA ≥2.0), Wilcoxon tests for panels (C,E,H) with FDR adjustment. *p < 0.05, **p < 0.01. All comparisons not specifically annotated were non-significant (ns). Mice were treated once daily for 14 days with DCZ (n = 6) or saline (n = 6).

chronic overactivation of this pathway may instead upregulate specific inflammatory factors [58]. TNF-α is primarily produced by activated macrophages and monocytes and its elevation suggests selective innate immune activation [59]. *Tnf* increase, without concurrent upregulation of T-cell-associated cytokines such as *Il12a*, may indicate selective activation of splenic myeloid cells. In addition, reduced *Il6* and *Il12a* may reflect adaptive immune suppression. IL-12a is critical for Th1 differentiation [60], and its decrease suggests impaired Th1-type adaptive immunity. Since Th1 cells activate other immune cells to eliminate pathogens, their decline may increase susceptibility

to intracellular pathogens, such as viruses and mycobacteria, due to impaired macrophage activation. This interpretation aligns with clinical observations in patients with chronic stress, who exhibit a state of "low-grade inflammation with impaired immune" function [61,62]. Moreover, stress is known to disrupt blood-brain-barrier (BBB), thereby increasing central nervous system (CNS) exposure to peripheral inflammatory factors. Our data further provide a plausible amygdala-spleen pathway through which cytokine-induced neuroinflammation may contribute to depression [63,64].

Acute stress typically elevates IL-22 as a rapid barrier-defense response preventing leaky gut syndrome, whereas patients with MDD and chronic-stress mouse models often exhibit lower IL-22 relative to controls. Moreover, exogenous IL-22 has been shown to reduce anxiety-like behavior in mice subjected to restraint stress [65]. IL-22 is also known to increase Reg3g expression via STAT3 signaling pathway and to support gut homeostasis [66,67]. In our chronically CeA^{CRH} activated mice, colonic IL-22 and Reg3g expression were both downregulated, consistent with observations in MDD or chronic stress conditions, suggesting impaired antimicrobial properties. Functionally, IL-22 promotes epithelial proliferation and renewal and differentially regulates mucins—upregulating MUC1 while downregulating MUC2 [67,68]. In addition, a recent study also indicates that CeA activation can stimulate Brunner's glands to secrete intestinal mucus. However, in our study, both mucins and tight-junction gene expression remained unchanged. This suggesting that CeA^{CRH} neurons may not directly control mucin releasing and IL-22 dependent changes in gut barrier gene expression change may be counteracted by other stress-responsive factors, such as hormonal or neuroimmune signals.

IL-22 is also known to induce Claudin-2 (Cldn2) via JAK/STAT signaling pathway [66,69], a cation-selective pore that increases paracellular permeability. We observed an increase in *Cldn2* expression in colon, which was somehow inconsistent with *Il22* decrease in CeA^{CRH} chronically activated mice. This finding implies that IL-22-independent or countervailing pathways should be engaged to increase gut permeability. Putative upstream pathways include TNF-α/NF-κB, EGFR–MEK/ERK, and TLR-mediated signaling, as well as reduced microbial SCFA abundance [70,71,72,73]. Despite the decreased CLDN-2 expression that pointing to impaired gut barrier function [69], our 4KD-Dextran test only exhibit a slightly increase of permeability in CeA^{CRH} activated mice. This may be partially due to the fact that Claudin2 do not permit the passage of large molecules such as dextran.

Gut permeability is closely associated with peripheral inflammatory status [74]. In contrast to the elevated inflammatory milieu commonly observed in chronic stress or MDD [6,73,75], selective activation of CeA^{CRH} neurons does not fully recapitulate this phenotype. Our data instead suggest reduced level of pro-inflammatory cytokines (IL-6, IL-2, TNF-α), indicating a defensive immune response typically associated with acute stress. This kind of low-level cytokine profile is plausible in our neuron-specifically activated mice, as chronic stress co-recruits multiple central and peripheral nodes (e.g., HPA axis, sympathetic outflow, BNST/hippocampus/mPFC), thereby producing more comprehensive systemic effects [76]. Notably, SCFA-producing bacteria reported to potentiate IL-22 signaling [77,78] were decreased in colonic contents in DCZ group (e.g., *Eubacterium siraeum* group and *Colidextribacter*). This finding suggests a potential microbiota → SCFA → IL-22/Reg3g axis, leading to compromised antimicrobial activity and gut barrier dysfunction. Consistent with this hypothesis, microbial-derived butyrate differentially regulates IL-22–dependent epithelial programs and facilitates mucosal recovery. In line with our random-forest analysis, the butyrate-producing *Roseburia*—a psychobiotic reported to enhance IL-22–mediated epithelial repair and alleviate symptoms in depression and long-term closed environment stress models [79,80]—was decreased in DCZ-treated mice. This finding further supports the idea that loss of SCFA may contribute to reduced IL-22/Reg3g expression and epithelial vulnerability. In addition, another study showed that disruption of GDNF–ILC3 signaling reduces IL-22, thereby exacerbating inflammation and increasing depression-like behavior [68].

Gut microbiota is a bidirectional communicator in the gut–brain axis, and can rapidly adapt to changes in physiological state within hours [11,81,82,83]. For instance, stress lowers mucosal defense, remodels epithelial milieu, and facilitates colonization by pathobionts such as AIEC (adherent-invasive Escherichia coli) [84]. CeA activation enhanced mucin secretion in Brunner's gland could also reshape the microbiome [24]. Although β-diversity between control and DCZ group were not intensely separated, we observed a compositional remodeling and evident changes at the functional level in metabolites or phenotypes [85]. In phylum level, Actinomycetota and Pseudomonadota are increased, indicating a micro-oxic, nitrate-permissive niche emerging from reduced butyrate-driven epithelial oxygen consumption—a pattern expected under chronic stress–mediated autonomic remodeling of the mucosal milieu.

Chronic or repeated stress is a well-established risk factor for MDD, involving contributions from both central neural circuits and peripheral pathways (autonomic, immune, and gut systems) [6,7,27]. Multiple studies have shown that individuals with MDD exhibit alterations in gut microbiome composition and function [86]. Given that hyperactivity of CeA has been reported in MDD patients [76,87,88], we hypothesized that selective activation of CeA^{CRH} neurons could induce similar microbiota those observed in MDD [40,41]. Thus we focus on 13 specific taxa identified in individuals with MDD and com-

pared them with our microbiome result [39,89]. Specifically, three taxa exhibited similar abundance changes in CeA^{CRH} activated mice while the remaining ten taxa were not detected in our study. An increasing number of animal studies have shown that the peripheral production of neurotransmitters by the gut microbiota can alter brain chemistry and therefore influence mood and behavior. Notably, *Eggerthella*, involved in the synthesis of serotonin and gamma aminobutyric acid, was increased in CeA^{CRH} activated cohort, suggesting a potential role in promoting mood disorders by gut-brain interaction [90,91,92]. Low GABA levels in the brain are closely linked to depression [93]. Although peripheral serotonin does not cross the BBB, gut-derived 5-HT can activate 5-HT_3 receptors on vagal afferents, thereby relaying signals to the brainstem and indirectly modulating central neurotransmission, including GABAergic tone. Moreover, microbiota-driven increases in enterochromaffin TPH1–dependent 5-HT, along with vagus-dependent changes in brain GABA receptor expression, further support its role in modulating central GABAergic activity [94,95].

Reciprocally, the observed microbiome profile in our study may also reflect the alteration of inflammation status: SCFA-producing taxa were diminished—exemplified by reduced *Roseburia* abundance, leading to reduced butyrate production, impaired gut barrier, anti-inflammatory signaling (GPCR/HDAC), and increased neuroinflammatory tone [96,97,98]. While small amounts of SCFAs (e.g., acetate and butyrate) can reach the brain, their primary anti-inflammatory effects are peripherally, where they stabilize the gut milieu (e.g., tight-junction support and IL-22/AMP programs) and modulate systemic immunity [77]. This kind of specific taxa alternation may contribute to be the transition from chronic stress exposure to depression by promoting peripheral inflammation.

Collectively, these findings delineate a CeA^{CRH}-driven suppression of the colonic IL-22–Reg3g axis, leading to impaired antimicrobial, gut barrier dysfunction and gut microbiota dysbiosis under chronic stress. Our study also identifies several potential therapeutic targets for stress induced gut dysfunction, as well as microbiota-based biomarker for the diagnosis of MDD.

Our study has some limitations. First, although we show activation of CeA^{CRH} neurons inhibit *Il22-Reg3g* levels in the colon, we did not investigate whether this modulation is mediated by direct downstream neural circuit or other indirect mechanism [99]. Retrograde trans-synaptic tracing approache, such as PRV, would be useful to further clarify the CeA-to-colon pathway. Second, the distinct cytokine gene expression patterns observed are not entirely consistent across typical serum cytokine level in stress paradigms. This discrepancy warrants further mechanistic investigation using time-course, tissue-resolved, and cell-type–specific analyses. In particular, flow cytometry would be valuable for verifying the functional status of specific subpopulations of immune cells. Third, the study was only performed exclusively in male mice. Given that females are generally more susceptible to stress-related disorders, sex-dependent effects should also be evaluated [100,101,102]. Last, while our results demonstrate that CeA^{CRH} activation reconfigures the microbiota into a depression-associated state, they do not establish direct causality. Futures studies employing fecal microbiota transplantation (FMT) in germ-free mice will be critical to determine if altered microbiota pattern is sufficient to drive the observed behavioral phenotypes and mucosal immune remodeling.

5. Conclusions

Chronic chemogenetic activation of CeA^{CRH} neurons induces suppressed colonic IL-22/Reg3g antimicrobial signaling, Claudin-2-dependent barrier disruption, and a microbiota profile alteration similar to depressed cohorts. Feedback from gut-to-brain may further reinforce central stress circuits and contribute to depression-related phenotypes. Our findings identify a potential top-down neuro–immune–microbiota mechanism linking amygdala activity to peripheral dysfunction, and highlight IL-22 restoration, barrier reinforcement or targeted microbiota modulation as potential therapeutic strategies for chronic stress.

Availability of Data and Materials

The 16S rRNA sequencing dataset can be accessed via the following link: https://www.ncbi.nlm.nih.gov/bioproject/?term=PRJNA1357088. Raw data is also available from the corresponding author upon reasonable request. Original code for behavioral analysis has been uploaded on Github (https://github.com/Liaorihong/Chemogenetic-activation-of-the-CeA-CRH.git).

Author Contributions

OF conceived the project and designed the experiments. LZ conducted all experiments, performed data acquisition and statistical analysis, and interpreted the results. YL established and optimized the RT-qPCR protocol, participated in RT-qPCR experiments, and analyzed the corresponding data. KZ and TQ participated in the experimental mouse husbandry, management, and daily i.p injection. SC and KZ participated in animal dissection, tissue collection, and brain slice preparation. OF and LZ wrote the original manuscript. All authors contributed to editorial changes in the manuscript. All authors read and approved the final manuscript. All authors have participated sufficiently in the work and agreed to be accountable for all aspects of the work.

Ethics Approval and Consent to Participate

All procedures and experiments on animals were performed according to the guidelines of Institutional Animal Care and Use Committees (IACUC) of Jiangnan Uni-

versity (SYXK 2021-0056, Ethics approval number: JN. No20241215t0140224 [638]). The study was conducted in accordance with the National Institutes of Health Guide for the Care and Use of Laboratory Animals.

Acknowledgment

We greatly appreciate Bohua Li from Beijing Normal University for his expert guidance on the implementation and training of the cell counting model and for his insightful recommendations regarding the behavioral analysis workflow. We thank Le Xu for providing the qPCR primers. We thank Liang Shen for his critique of the manuscript.

Funding

This study was supported by grants from Natural Science Foundation of China (32400838 and 32571190) and Basic Research Program of Jiangsu (BK20231046).

Conflicts of Interest

The authors declare no conflicts of interest.

Declaration of AI and AI-Assisted Technologies in the Writing Process

The authors used an AI-assisted tool (ChatGPT, OpenAI) only for language editing and polishing. All content was reviewed and verified by the authors, who take full responsibility for the manuscript's accuracy and integrity. No patient/identifiable data were entered into the tool.

Supplementary Material

Supplementary material associated with this article can be found, in the online version, at https://doi.org/10.31083/JIN48170.

References

[1] Shouman K, Benarroch EE. Peripheral neuroimmune interactions: selected review and some clinical implications. Clinical Autonomic Research : Official Journal of the Clinical Autonomic Research Society. 2021; 31: 477–489. https://doi.org/10.1007/s10286-021-00787-5

[2] Izumi M, Nakanishi Y, Kang S, Kumanogoh A. Peripheral and central regulation of neuro-immune crosstalk. Inflammation and Regeneration. 2024; 44: 41. https://doi.org/10.1186/s41232-024-00352-3

[3] Andersson U, Tracey KJ. Neural reflexes in inflammation and immunity. The Journal of Experimental Medicine. 2012; 209: 1057–1068. https://doi.org/10.1084/jem.20120571

[4] Dantzer R. Neuroimmune Interactions: From the Brain to the Immune System and Vice Versa. Physiological Reviews. 2018; 98: 477–504. https://doi.org/10.1152/physrev.00039.2016

[5] Jin H, Li M, Jeong E, Castro-Martinez F, Zuker CS. A body-brain circuit that regulates body inflammatory responses. Nature. 2024; 630: 695–703. https://doi.org/10.1038/s41586-024-07469-y

[6] Schneider KM, Blank N, Alvarez Y, Thum K, Lundgren P, Litichevskiy L, et al. The enteric nervous system relays psychological stress to intestinal inflammation. Cell. 2023; 186: 2823–2838.e20. https://doi.org/10.1016/j.cell.2023.05.001

[7] Feng X, Jia M, Cai M, Zhu T, Hashimoto K, Yang JJ. Central-peripheral neuroimmune dynamics in psychological stress and depression: insights from current research. Molecular Psychiatry. 2025; 30: 4881–4898. https://doi.org/10.1038/s41380-025-03085-y

[8] Madison AA, Bailey MT. Stressed to the Core: Inflammation and Intestinal Permeability Link Stress-Related Gut Microbiota Shifts to Mental Health Outcomes. Biological Psychiatry. 2024; 95: 339–347. https://doi.org/10.1016/j.biopsych.2023.10.014

[9] Morais LH, Schreiber HL, 4th, Mazmanian SK. The gut microbiota-brain axis in behaviour and brain disorders. Nature Reviews. Microbiology. 2021; 19: 241–255. https://doi.org/10.1038/s41579-020-00460-0

[10] Ohara TE, Hsiao EY. Microbiota-neuroepithelial signalling across the gut-brain axis. Nature Reviews. Microbiology. 2025; 23: 371–384. https://doi.org/10.1038/s41579-024-01136-9

[11] Toledo M, Martínez-Martínez S, Van Hul M, Laudo B, Eyre E, Pelicaen R, et al. Rapid modulation of gut microbiota composition by hypothalamic circuits in mice. Nature Metabolism. 2025; 7: 1123–1135. https://doi.org/10.1038/s42255-025-01280-3

[12] Ben-Shaanan TL, Schiller M, Azulay-Debby H, Korin B, Boshnak N, Koren T, et al. Modulation of anti-tumor immunity by the brain's reward system. Nature Communications. 2018; 9: 2723. https://doi.org/10.1038/s41467-018-05283-5

[13] Afridi R, Seol S, Kang HJ, Suk K. Brain-immune interactions in neuropsychiatric disorders: Lessons from transcriptome studies for molecular targeting. Biochemical Pharmacology. 2021; 188: 114532. https://doi.org/10.1016/j.bcp.2021.114532

[14] Segan L, Prabhu S, Kalman JM, Kistler PM. Atrial Fibrillation and Stress: A 2-Way Street? JACC. Clinical Electrophysiology. 2022; 8: 1051–1059. https://doi.org/10.1016/j.jacep.2021.12.008

[15] Araki M, Shinzaki S, Yamada T, Arimitsu S, Komori M, Shibukawa N, et al. Psychologic stress and disease activity in patients with inflammatory bowel disease: A multicenter cross-sectional study. PloS One. 2020; 15: e0233365. https://doi.org/10.1371/journal.pone.0233365

[16] Payne JL, Maguire J. Pathophysiological mechanisms implicated in postpartum depression. Frontiers in Neuroendocrinology. 2019; 52: 165–180. https://doi.org/10.1016/j.yfrne.2018.12.001

[17] Kong MS, Zweifel LS. Central amygdala circuits in valence and salience processing. Behavioural Brain Research. 2021; 410: 113355. https://doi.org/10.1016/j.bbr.2021.113355

[18] Li J, Li ZA, Tian HM, Tao SS, Zhang Q, Li F, et al. Corticotropin-releasing hormone neurons in the central Amygdala: An integrative hub for pain, emotion, and addiction neurobiology. Brain Research. 2025; 1863: 149753. https://doi.org/10.1016/j.brainres.2025.149753

[19] McCullough KM, Chatzinakos C, Hartmann J, Missig G, Neve RL, Fenster RJ, et al. Genome-wide translational profiling of amygdala Crh-expressing neurons reveals role for CREB in fear extinction learning. Nature Communications. 2020; 11: 5180. https://doi.org/10.1038/s41467-020-18985-6

[20] Veinante P, Yalcin I, Barrot M. The amygdala between sensation and affect: a role in pain. Journal of Molecular Psychiatry. 2013; 1: 9. https://doi.org/10.1186/2049-9256-1-9

[21] Paretkar T, Dimitrov E. The Central Amygdala Corticotropin-releasing hormone (CRH) Neurons Modulation of Anxiety-like Behavior and Hippocampus-dependent Memory in Mice. Neuroscience. 2018; 390: 187–197. https://doi.org/10.1016/j.neuroscience.2018.08.019

[22] Zhu X, Huang JY, Dong WY, Tang HD, Xu S, Wu Q, et al. Somatosensory cortex and central amygdala regulate neuropathic pain-mediated peripheral immune response via vagal projec-

tions to the spleen. Nature Neuroscience. 2024; 27: 471–483. https://doi.org/10.1038/s41593-023-01561-8
[23] Zhang X, Lei B, Yuan Y, Zhang L, Hu L, Jin S, et al. Brain control of humoral immune responses amenable to behavioural modulation. Nature. 2020; 581: 204–208. https://doi.org/10.1038/s41586-020-2235-7
[24] Chang H, Perkins MH, Novaes LS, Qian F, Zhang T, Neckel PH, et al. Stress-sensitive neural circuits change the gut microbiome via duodenal glands. Cell. 2024; 187: 5393–5412.e30. https://doi.org/10.1016/j.cell.2024.07.019
[25] Mayer EA, Ryu HJ, Bhatt RR. The neurobiology of irritable bowel syndrome. Molecular Psychiatry. 2023; 28: 1451–1465. https://doi.org/10.1038/s41380-023-01972-w
[26] Rogers GB, Keating DJ, Young RL, Wong ML, Licinio J, Wesselingh S. From gut dysbiosis to altered brain function and mental illness: mechanisms and pathways. Molecular Psychiatry. 2016; 21: 738–748. https://doi.org/10.1038/mp.2016.50
[27] Xu Q, Sun L, Chen Q, Jiao C, Wang Y, Li H, et al. Gut microbiota dysbiosis contributes to depression-like behaviors via hippocampal NLRP3-mediated neuroinflammation in a postpartum depression mouse model. Brain, Behavior, and Immunity. 2024; 119: 220–235. https://doi.org/10.1016/j.bbi.2024.04.002
[28] Nagai Y, Miyakawa N, Takuwa H, Hori Y, Oyama K, Ji B, et al. Deschloroclozapine, a potent and selective chemogenetic actuator enables rapid neuronal and behavioral modulations in mice and monkeys. Nature Neuroscience. 2020; 23: 1157–1167. https://doi.org/10.1038/s41593-020-0661-3
[29] Mathis A, Mamidanna P, Cury KM, Abe T, Murthy VN, Mathis MW, et al. DeepLabCut: markerless pose estimation of user-defined body parts with deep learning. Nature Neuroscience. 2018; 21: 1281–1289. https://doi.org/10.1038/s41593-018-0209-y
[30] Shin NR, Whon TW, Bae JW. Proteobacteria: microbial signature of dysbiosis in gut microbiota. Trends in Biotechnology. 2015; 33: 496–503. https://doi.org/10.1016/j.tibtech.2015.06.011
[31] Rizzatti G, Lopetuso LR, Gibiino G, Binda C, Gasbarrini A. Proteobacteria: A Common Factor in Human Diseases. BioMed Research International. 2017; 2017: 9351507. https://doi.org/10.1155/2017/9351507
[32] Barandouzi ZA, Starkweather AR, Henderson WA, Gyamfi A, Cong XS. Altered Composition of Gut Microbiota in Depression: A Systematic Review. Frontiers in Psychiatry. 2020; 11: 541. https://doi.org/10.3389/fpsyt.2020.00541
[33] Zhou Y, Zhang F, Mao L, Feng T, Wang K, Xu M, et al. Bifico relieves irritable bowel syndrome by regulating gut microbiota dysbiosis and inflammatory cytokines. European Journal of Nutrition. 2023; 62: 139–155. https://doi.org/10.1007/s00394-022-02958-0
[34] Lyte M. Microbial Endocrinology in the Pathogenesis of Infectious Disease. Microbiology Spectrum. 2016; 4. https://doi.org/10.1128/microbiolspec.VMBF-0021-2015
[35] Liu C, Chi K, Yang M, Guo N. Staphylococcal Enterotoxin A Induces Intestinal Barrier Dysfunction and Activates NLRP3 Inflammasome via NF-κB/MAPK Signaling Pathways in Mice. Toxins. 2022; 14: 29. https://doi.org/10.3390/toxins14010029
[36] Kamada N, Seo SU, Chen GY, Núñez G. Role of the gut microbiota in immunity and inflammatory disease. Nature Reviews. Immunology. 2013; 13: 321–335. https://doi.org/10.1038/nri3430
[37] Valles-Colomer M, Falony G, Darzi Y, Tigchelaar EF, Wang J, Tito RY, et al. The neuroactive potential of the human gut microbiota in quality of life and depression. Nature Microbiology. 2019; 4: 623–632. https://doi.org/10.1038/s41564-018-0337-x
[38] Tamanai-Shacoori Z, Smida I, Bousarghin L, Loreal O, Meuric V, Fong SB, et al. Roseburia spp.: a marker of health? Future Microbiology. 2017; 12: 157–170. https://doi.org/10.2217/fmb-2016-0130
[39] Radjabzadeh D, Bosch JA, Uitterlinden AG, Zwinderman AH, Ikram MA, van Meurs JBJ, et al. Gut microbiome-wide association study of depressive symptoms. Nature Communications. 2022; 13: 7128. https://doi.org/10.1038/s41467-022-34502-3
[40] Gao M, Wang J, Liu P, Tu H, Zhang R, Zhang Y, et al. Gut microbiota composition in depressive disorder: a systematic review, meta-analysis, and meta-regression. Translational Psychiatry. 2023; 13: 379. https://doi.org/10.1038/s41398-023-02670-5
[41] Simpson CA, Diaz-Arteche C, Eliby D, Schwartz OS, Simmons JG, Cowan CSM. The gut microbiota in anxiety and depression - A systematic review. Clinical Psychology Review. 2021; 83: 101943. https://doi.org/10.1016/j.cpr.2020.101943
[42] Liu L, Wang H, Chen X, Zhang Y, Zhang H, Xie P. Gut microbiota and its metabolites in depression: from pathogenesis to treatment. eBioMedicine. 2023; 90: 104527. https://doi.org/10.1016/j.ebiom.2023.104527
[43] Wu Y, Sun F, Guo Y, Zhang Y, Li L, Dang R, et al. Curcumin Relieves Chronic Unpredictable Mild Stress-Induced Depression-Like Behavior through the PGC-1α/FNDC5/BDNF Pathway. Behavioural Neurology. 2021; 2021: 2630445. https://doi.org/10.1155/2021/2630445
[44] Qiao Y, Zhao J, Li C, Zhang M, Wei L, Zhang X, et al. Effect of combined chronic predictable and unpredictable stress on depression-like symptoms in mice. Annals of Translational Medicine. 2020; 8: 942. https://doi.org/10.21037/atm-20-5168
[45] Radley J, Morilak D, Viau V, Campeau S. Chronic stress and brain plasticity: Mechanisms underlying adaptive and maladaptive changes and implications for stress-related CNS disorders. Neuroscience and Biobehavioral Reviews. 2015; 58: 79–91. https://doi.org/10.1016/j.neubiorev.2015.06.018
[46] Aguilera-Lizarraga J, Lopez-Lopez C, Jaramillo-Polanco J, Florens MV, Yu Y, Tsang QK, et al. Psychological Stress-Induced Local Immune Response to Food Antigens Increases Pain Signaling Across the Gut in Mice. Gastroenterology. 2025; 169: 104–118.e4. https://doi.org/10.1053/j.gastro.2025.01.246
[47] Shin LM, Liberzon I. The neurocircuitry of fear, stress, and anxiety disorders. Neuropsychopharmacology : Official Publication of the American College of Neuropsychopharmacology. 2010; 35: 169–191. https://doi.org/10.1038/npp.2009.83
[48] Sanford CA, Soden ME, Baird MA, Miller SM, Schulkin J, Palmiter RD, et al. A Central Amygdala CRF Circuit Facilitates Learning about Weak Threats. Neuron. 2017; 93: 164–178. https://doi.org/10.1016/j.neuron.2016.11.034
[49] Wang SS, Yan XB, Hofman MA, Swaab DF, Zhou JN. Increased expression level of corticotropin-releasing hormone in the amygdala and in the hypothalamus in rats exposed to chronic unpredictable mild stress. Neuroscience Bulletin. 2010; 26: 297–303. https://doi.org/10.1007/s12264-010-0329-1
[50] Chakrabarty T, Hadjipavlou G, Lam RW. Cognitive Dysfunction in Major Depressive Disorder: Assessment, Impact, and Management. Focus (American Psychiatric Publishing). 2016; 14: 194–206. https://doi.org/10.1176/appi.focus.20150043
[51] Rock PL, Roiser JP, Riedel WJ, Blackwell AD. Cognitive impairment in depression: a systematic review and meta-analysis. Psychological Medicine. 2014; 44: 2029–2040. https://doi.org/10.1017/S0033291713002535
[52] Mazzitelli M, Yakhnitsa V, Neugebauer B, Neugebauer V. Optogenetic manipulations of CeA-CRF neurons modulate pain- and anxiety-like behaviors in neuropathic pain and control rats. Neuropharmacology. 2022; 210: 109031. https://doi.org/10.1016/j.neuropharm.2022.109031
[53] Bao AM, Meynen G, Swaab DF. The stress system in depression and neurodegeneration: focus on the human hypothalamus. Brain Research Reviews. 2008; 57: 531–553. https://doi.org/10.

1016/j.brainresrev.2007.04.005
[54] Dallman MF, Pecoraro N, Akana SF, La Fleur SE, Gomez F, Houshyar H, et al. Chronic stress and obesity: a new view of "comfort food". Proceedings of the National Academy of Sciences of the United States of America. 2003; 100: 11696–11701. https://doi.org/10.1073/pnas.1934666100
[55] Dallman MF. Stress-induced obesity and the emotional nervous system. Trends in Endocrinology and Metabolism: TEM. 2010; 21: 159–165. https://doi.org/10.1016/j.tem.2009.10.004
[56] Montgomery KR, Bridi MS, Folts LM, Marx-Rattner R, Zierden HC, Wulff AB, et al. Chemogenetic activation of CRF neurons as a model of chronic stress produces sex-specific physiological and behavioral effects. Neuropsychopharmacology : Official Publication of the American College of Neuropsychopharmacology. 2024; 49: 443–454. https://doi.org/10.1038/s41386-023-01739-5
[57] Mota CMD, Madden CJ. Neural control of the spleen as an effector of immune responses to inflammation: mechanisms and treatments. American Journal of Physiology. Regulatory, Integrative and Comparative Physiology. 2022; 323: R375–R384. https://doi.org/10.1152/ajpregu.00151.2022
[58] Leigh SJ, Uhlig F, Wilmes L, Sanchez-Diaz P, Gheorghe CE, Goodson MS, et al. The impact of acute and chronic stress on gastrointestinal physiology and function: a microbiota-gut-brain axis perspective. The Journal of Physiology. 2023; 601: 4491–4538. https://doi.org/10.1113/JP281951
[59] Parameswaran N, Patial S. Tumor necrosis factor-α signaling in macrophages. Critical Reviews in Eukaryotic Gene Expression. 2010; 20: 87–103. https://doi.org/10.1615/critreveukargeneexpr.v20.i2.10
[60] Trinchieri G. Interleukin-12 and the regulation of innate resistance and adaptive immunity. Nature Reviews. Immunology. 2003; 3: 133–146. https://doi.org/10.1038/nri1001
[61] Dhabhar FS. Effects of stress on immune function: the good, the bad, and the beautiful. Immunologic Research. 2014; 58: 193–210. https://doi.org/10.1007/s12026-014-8517-0
[62] Segerstrom SC, Miller GE. Psychological stress and the human immune system: a meta-analytic study of 30 years of inquiry. Psychological Bulletin. 2004; 130: 601–630. https://doi.org/10.1037/0033-2909.130.4.601
[63] Menard C, Pfau ML, Hodes GE, Kana V, Wang VX, Bouchard S, et al. Social stress induces neurovascular pathology promoting depression. Nature Neuroscience. 2017; 20: 1752–1760. https://doi.org/10.1038/s41593-017-0010-3
[64] Hassamal S. Chronic stress, neuroinflammation, and depression: an overview of pathophysiological mechanisms and emerging anti-inflammatories. Frontiers in Psychiatry. 2023; 14: 1130989. https://doi.org/10.3389/fpsyt.2023.1130989
[65] Xia M, Lu J, Lan J, Teng T, Shiao R, Sun H, et al. Elevated IL-22 as a result of stress-induced gut leakage suppresses septal neuron activation to ameliorate anxiety-like behavior. Immunity. 2025; 58: 218–231.e12. https://doi.org/10.1016/j.immuni.2024.11.008
[66] Hammer AM, Morris NL, Cannon AR, Khan OM, Gagnon RC, Movtchan NV, et al. Interleukin-22 Prevents Microbial Dysbiosis and Promotes Intestinal Barrier Regeneration Following Acute Injury. Shock (Augusta, Ga.). 2017; 48: 657–665. https://doi.org/10.1097/SHK.0000000000000900
[67] Patnaude L, Mayo M, Mario R, Wu X, Knight H, Creamer K, et al. Mechanisms and regulation of IL-22-mediated intestinal epithelial homeostasis and repair. Life Sciences. 2021; 271: 119195. https://doi.org/10.1016/j.lfs.2021.119195
[68] Singh A, Beaupre M, Villegas-Novoa C, Shiomitsu K, Gaudino SJ, Tawch S, et al. IL-22 promotes mucin-type O-glycosylation and MATH1$^+$ cell-mediated amelioration of intestinal inflammation. Cell Reports. 2024; 43: 114206. https://doi.org/10.1016/j.celrep.2024.114206
[69] Tsai PY, Zhang B, He WQ, Zha JM, Odenwald MA, Singh G, et al. IL-22 Upregulates Epithelial Claudin-2 to Drive Diarrhea and Enteric Pathogen Clearance. Cell Host & Microbe. 2017; 21: 671–681.e4. https://doi.org/10.1016/j.chom.2017.05.009
[70] Liu L, Zhu G. Gut-Brain Axis and Mood Disorder. Frontiers in psychiatry. 2018; 9: 223. https://doi.org/10.3389/fpsyt.2018.00223
[71] Ma TY, Iwamoto GK, Hoa NT, Akotia V, Pedram A, Boivin MA, et al. TNF-alpha-induced increase in intestinal epithelial tight junction permeability requires NF-kappa B activation. American Journal of Physiology. Gastrointestinal and Liver Physiology. 2004; 286: G367–76. https://doi.org/10.1152/ajpgi.00173.2003
[72] Ikari A, Sato T, Watanabe R, Yamazaki Y, Sugatani J. Increase in claudin-2 expression by an EGFR/MEK/ERK/c-Fos pathway in lung adenocarcinoma A549 cells. Biochimica et Biophysica Acta. 2012; 1823: 1110–1118. https://doi.org/10.1016/j.bbamcr.2012.04.005
[73] Luo H, Guo P, Zhou Q. Role of TLR4/NF-κB in damage to intestinal mucosa barrier function and bacterial translocation in rats exposed to hypoxia. PloS One. 2012; 7: e46291. https://doi.org/10.1371/journal.pone.0046291
[74] Agirman G, Yu KB, Hsiao EY. Signaling inflammation across the gut-brain axis. Science (New York, N.Y.). 2021; 374: 1087–1092. https://doi.org/10.1126/science.abi6087
[75] do Sacramento PM, Sales M, Kasahara TDM, Monteiro C, Oyamada H, Dias ASO, et al. Major depression favors the expansion of Th17-like cells and decrease the proportion of CD39$^+$Treg cell subsets in response to myelin antigen in multiple sclerosis patients. Cellular and Molecular Life Sciences : CMLS. 2022; 79: 298. https://doi.org/10.1007/s00018-022-04315-0
[76] Ressler KJ, Mayberg HS. Targeting abnormal neural circuits in mood and anxiety disorders: from the laboratory to the clinic. Nature Neuroscience. 2007; 10: 1116–1124. https://doi.org/10.1038/nn1944
[77] Liu XF, Shao JH, Liao YT, Wang LN, Jia Y, Dong PJ, et al. Regulation of short-chain fatty acids in the immune system. Frontiers in Immunology. 2023; 14: 1186892. https://doi.org/10.3389/fimmu.2023.1186892
[78] Bachmann M, Meissner C, Pfeilschifter J, Mühl H. Cooperation between the bacterial-derived short-chain fatty acid butyrate and interleukin-22 detected in human Caco2 colon epithelial/carcinoma cells. BioFactors (Oxford, England). 2017; 43: 283–292. https://doi.org/10.1002/biof.1341
[79] Hao Z, Meng C, Li L, Feng S, Zhu Y, Yang J, et al. Positive mood-related gut microbiota in a long-term closed environment: a multiomics study based on the "Lunar Palace 365" experiment. Microbiome. 2023; 11: 88. https://doi.org/10.1186/s40168-023-01506-0
[80] Zhao M, Ren Z, Zhao A, Tang Y, Kuang J, Li M, et al. Gut bacteria-driven homovanillic acid alleviates depression by modulating synaptic integrity. Cell Metabolism. 2024; 36: 1000–1012.e6. https://doi.org/10.1016/j.cmet.2024.03.010
[81] Madison A, Kiecolt-Glaser JK. Stress, depression, diet, and the gut microbiota: human-bacteria interactions at the core of psychoneuroimmunology and nutrition. Current Opinion in Behavioral Sciences. 2019; 28: 105–110. https://doi.org/10.1016/j.cobeha.2019.01.011
[82] Montagnani M, Bottalico L, Potenza MA, Charitos IA, Topi S, Colella M, et al. The Crosstalk between Gut Microbiota and Nervous System: A Bidirectional Interaction between Microorganisms and Metabolome. International Journal of Molecular Sciences. 2023; 24: 10322. https://doi.org/10.3390/ijms241210322
[83] Yuan C, He Y, Xie K, Feng L, Gao S, Cai L. Review of microbiota gut brain axis and innate immunity in inflammatory and

infective diseases. Frontiers in Cellular and Infection Microbiology. 2023; 13: 1282431. https://doi.org/10.3389/fcimb.2023.1282431

[84] Shaler CR, Parco AA, Elhenawy W, Dourka J, Jury J, Verdu EF, et al. Psychological stress impairs IL22-driven protective gut mucosal immunity against colonising pathobionts. Nature Communications. 2021; 12: 6664. https://doi.org/10.1038/s41467-021-26992-4

[85] Zheng KY, Gao B, Wang HJ, He JG, Chen HS, Hu ZL, et al. Melatonin Ameliorates Depressive-Like Behaviors in Ovariectomized Mice by Improving Tryptophan Metabolism via Inhibition of Gut Microbe Alistipes Inops. Advanced Science (Weinheim, Baden-Wurttemberg, Germany). 2024; 11: e2309473. https://doi.org/10.1002/advs.202309473

[86] Foster JA, Rinaman L, Cryan JF. Stress & the gut-brain axis: Regulation by the microbiome. Neurobiology of Stress. 2017; 7: 124–136. https://doi.org/10.1016/j.ynstr.2017.03.001

[87] Yang TT, Simmons AN, Matthews SC, Tapert SF, Frank GK, Max JE, et al. Adolescents with major depression demonstrate increased amygdala activation. Journal of the American Academy of Child and Adolescent Psychiatry. 2010; 49: 42–51. https://doi.org/10.1097/00004583-201001000-00008

[88] Loureiro JRA, Leaver A, Vasavada M, Sahib AK, Kubicki A, Joshi S, et al. Modulation of amygdala reactivity following rapidly acting interventions for major depression. Human Brain Mapping. 2020; 41: 1699–1710. https://doi.org/10.1002/hbm.24895

[89] Huang Y, Shi X, Li Z, Shen Y, Shi X, Wang L, et al. Possible association of Firmicutes in the gut microbiota of patients with major depressive disorder. Neuropsychiatric Disease and Treatment. 2018; 14: 3329–3337. https://doi.org/10.2147/NDT.S188340

[90] Wong AC, Devason AS, Umana IC, Cox TO, Dohnalová L, Litichevskiy L, et al. Serotonin reduction in post-acute sequelae of viral infection. Cell. 2023; 186: 4851–4867.e20. https://doi.org/10.1016/j.cell.2023.09.013

[91] Gao K, Mu CL, Farzi A, Zhu WY. Tryptophan Metabolism: A Link Between the Gut Microbiota and Brain. Advances in Nutrition (Bethesda, Md.). 2020; 11: 709–723. https://doi.org/10.1093/advances/nmz127

[92] Reigstad CS, Salmonson CE, Rainey JF, 3rd, Szurszewski JH, Linden DR, Sonnenburg JL, et al. Gut microbes promote colonic serotonin production through an effect of short-chain fatty acids on enterochromaffin cells. FASEB Journal : Official Publication of the Federation of American Societies for Experimental Biology. 2015; 29: 1395–1403. https://doi.org/10.1096/fj.14-259598

[93] Lydiard RB. The role of GABA in anxiety disorders. The Journal of Clinical Psychiatry. 2003; 64 Suppl 3: 21–27.

[94] O'Mahony SM, Clarke G, Borre YE, Dinan TG, Cryan JF. Serotonin, tryptophan metabolism and the brain-gut-microbiome axis. Behavioural Brain Research. 2015; 277: 32–48. https://doi.org/10.1016/j.bbr.2014.07.027

[95] Goggins E, Mitani S, Tanaka S. Clinical perspectives on vagus nerve stimulation: present and future. Clinical Science (London, England : 1979). 2022; 136: 695–709. https://doi.org/10.1042/CS20210507

[96] Caspani G, Kennedy S, Foster JA, Swann J. Gut microbial metabolites in depression: understanding the biochemical mechanisms. Microbial Cell (Graz, Austria). 2019; 6: 454–481. https://doi.org/10.15698/mic2019.10.693

[97] de Clercq NC, Groen AK, Romijn JA, Nieuwdorp M. Gut Microbiota in Obesity and Undernutrition. Advances in Nutrition (Bethesda, Md.). 2016; 7: 1080–1089. https://doi.org/10.3945/an.116.012914

[98] Mason BL, Li Q, Minhajuddin A, Czysz AH, Coughlin LA, Hussain SK, et al. Reduced anti-inflammatory gut microbiota are associated with depression and anhedonia. Journal of Affective Disorders. 2020; 266: 394–401. https://doi.org/10.1016/j.jad.2020.01.137

[99] Adke AP, Khan A, Ahn HS, Becker JJ, Wilson TD, Valdivia S, et al. Cell-Type Specificity of Neuronal Excitability and Morphology in the Central Amygdala. eNeuro. 2021; 8: ENEURO.0402–20.2020. https://doi.org/10.1523/ENEURO.0402-20.2020

[100] Effinger DP, Quadir SG, Ramage MC, Cone MG, Herman MA. Sex-specific effects of psychedelic drug exposure on central amygdala reactivity and behavioral responding. Translational Psychiatry. 2023; 13: 119. https://doi.org/10.1038/s41398-023-02414-5

[101] Hodes GE, Bangasser D, Sotiropoulos I, Kokras N, Dalla C. Sex Differences in Stress Response: Classical Mechanisms and Beyond. Current Neuropharmacology. 2024; 22: 475–494. https://doi.org/10.2174/1570159X22666231005090134

[102] Rybka KA, Lafrican JJ, Rosinger ZJ, Ariyibi DO, Brooks MR, Jacobskind JS, et al. Sex differences in androgen receptor, estrogen receptor alpha, and c-Fos co-expression with corticotropin releasing factor expressing neurons in restrained adult mice. Hormones and Behavior. 2023; 156: 105448. https://doi.org/10.1016/j.yhbeh.2023.105448